

## Article

# The Effects of Plant and Soil Characteristics on Partitioning Different Rainfalls to Soil in a Subtropical Chinese Fir Forest Ecosystem

Ying Zhang<sup>1</sup>, Beibei Zhang<sup>1</sup>, Qing Xu<sup>1,\*</sup>, Deqiang Gao<sup>1</sup>, Wenbin Xu<sup>1</sup>, Ranran Ren<sup>1</sup>, Jing Jiang<sup>2</sup>   
and Silong Wang<sup>3</sup>

<sup>1</sup> Key Laboratory of Forest Ecology and Environment of National Forestry and Grassland Administration, Institute of Forest Ecology, Environment and Nature Conservation, Chinese Academy of Forestry, Beijing 100091, China; cherrycedar@163.com (Y.Z.); zhangbb@caf.ac.cn (B.Z.); gaodeqiang@caf.ac.cn (D.G.); xuwenbin@caf.ac.cn (W.X.); xiaoran2822@163.com (R.R.)

<sup>2</sup> Department of Forest and Conservation Sciences, Faculty of Forestry, University of British Columbia, Vancouver, BC V6T 1Z4, Canada; jing007@student.ubc.ca

<sup>3</sup> Huitong National Research Station of Forest Ecosystem, Institute of Applied Ecology, Chinese Academy of Sciences, Shenyang 110016, China; slwang21@126.com

\* Correspondence: xuqing@caf.ac.cn; Tel.: +86-10-6288-9549

**Abstract:** The climate-induced changes in soil water patterns pose a serious threat to subtropical plantations. Mixed species stands have been advocated as an efficient way to enhance ecosystem stability. However, little is known about their possible impact on the soil water-holding capacity in the subtropics. In this study, we employed a stable hydrogen isotope to assess the contribution of rainfall to soil water (CRSW) in a pure Chinese fir (*Cunninghamia lanceolata*) plantation and in two mixtures of Chinese fir with *Cinnamomum camphora* or with *Alnus cremastogyne* after three different magnitudes of rainfall events in subtropical China. Furthermore, we used structure equation modeling (SEM) to quantify the relative importance of vegetation and soil properties on the CRSW. The results indicated that the CRSW did not differ among these three Chinese fir plantations after light rainfall, whereas the CRSW of moderate and heavy rainfall to soil water were 15.95% and 26.06% higher in Chinese fir plantation with *Cinnamomum camphora*, and 22.67% and 22.93% higher in Chinese fir plantation with *Alnus cremastogyne* than that in the pure Chinese fir plantation, respectively. SEM analysis showed that the vegetation biomass and soil properties significantly affected the CRSW following light rainfall, but the soil properties were the most important factors influencing the CRSW under moderate and heavy rainfall. Our findings demonstrate that the mixed conifer–broad-leaved plantation is a more effective strategy for improving the soil water-holding capacity than the pure conifer plantation in subtropical regions, which is conducive to coping with the frequent seasonal droughts and extreme precipitation events.

**Keywords:** stable hydrogen isotope; precipitation; mixed plantations; soil water; Chinese fir



**Citation:** Zhang, Y.; Zhang, B.; Xu, Q.; Gao, D.; Xu, W.; Ren, R.; Jiang, J.; Wang, S. The Effects of Plant and Soil Characteristics on Partitioning Different Rainfalls to Soil in a Subtropical Chinese Fir Forest Ecosystem. *Forests* **2022**, *13*, 123. <https://doi.org/10.3390/f13010123>

Academic Editor: Francisco B. Navarro

Received: 1 December 2021

Accepted: 11 January 2022

Published: 14 January 2022

**Publisher's Note:** MDPI stays neutral with regard to jurisdictional claims in published maps and institutional affiliations.



**Copyright:** © 2022 by the authors. Licensee MDPI, Basel, Switzerland. This article is an open access article distributed under the terms and conditions of the Creative Commons Attribution (CC BY) license (<https://creativecommons.org/licenses/by/4.0/>).

## 1. Introduction

Soil water, ecohydrologically linking rainfall, surface water and groundwater, is a central component of the hydrological cycle [1–3]. Additionally, soil water plays an essential role in the coupling and feedback of vegetation–soil systems [4]. It determines the spatiotemporal distribution and ecological function of vegetation by affecting various physical and biogeochemical processes, such as carbon–nitrogen cycling, plant growth and microbial activity [5,6]. Considering the impact of global changes on precipitation regimes, extreme precipitation and seasonal drought events are likely to become more intense and frequent in the future [7–9], which will significantly affect the stability of soil water dynamics and forest ecosystems. Therefore, a better understanding of the response mechanisms of soil water to rainfall is essential for predicting and maintaining the sustainability of forest ecosystems.

Precipitation exerts a critical role on soil water dynamics owing to its decisive effect on water distribution. However, vegetation can also effectively regulate soil water dynamics by participating in various hydrological processes [10,11]. Plants can affect soil water dynamics through mediating rainfall redistribution, leaf interception and runoff [3,12]. On the other hand, plants can control soil water evaporation by root uptake [13]. Nevertheless, their impact on soil water dynamics can vary based on the vegetation type, composition and structure [4,14]. As a vital forest type, the eco-function of mixed species forests is increasingly valued in the context of climate change and resource scarcity [15,16]. There is increasing evidence that mixed forests have the potential to enhance ecosystem productivity and carbon sequestration, as well as having a higher resistance and resilience against the changing climate conditions [17,18]. In terms of soil water dynamics, some studies have reported that mixed and coexisting species can promote the allocation of precipitation to soil water through increasing root biomass and shaping litter hydrological characteristics [19]. However, mixed plantations can also have negative effects on soil water dynamics. Larger canopies and multigroup composite structures can result in greater rainfall interception and evaporative water loss compared to those for monocultures [20]. As a result of the multiple complex and interactive feedback mechanisms between vegetation and soil water, it is unclear whether mixed plantations have a positive impact on soil water dynamics. Furthermore, the effect of plantation types (i.e., mixed plantations and monocultures) on soil water-holding under different precipitation conditions is often neglected under the global climate change scenario, especially in humid subtropical regions.

Soil water dynamic, as the consequence of complex and mutually hydrological interactions, is impacted by multiple factors [21–26]. In general, forest soil water dynamics are determined by vegetation and soil properties. As an important water pool, soil plays a crucial role in the soil water dynamics of terrestrial ecosystems [21–23]. Favorable soil properties (i.e., soil texture, bulk density or soil porosity) help to improve precipitation infiltration and possess a higher water-holding capacity [22,24], which significantly affects the soil water content. Hence, soil properties are considered as the main direct factor controlling the soil water dynamics of forests. However, a growing number of studies have shown that soil water dynamics are more prone to being impacted by the vegetation characteristics [25,26]. The interception and redistribution of precipitation by above-ground vegetation and litter mediate the rainfall reaching into the soil, which can contribute to the difference in the soil water dynamics between pure and mixed forest stands [27,28]. Moreover, the plant root system plays an important role in modifying soil water dynamics at the root–soil interface [29]. The vertical profile of the root biomass of plants directly or indirectly impacts the soil hydraulic conductivity and infiltration processes, which in turn influence soil water dynamics [30,31]. Overall, though many studies have reported the factors related to soil water dynamics, how vegetation and soil properties and their interactions drive the changes in soil water dynamics under different plantation types is not well understood.

Recent studies have suggested that subtropical forests are threatened by their lack of resilience against climate change [32,33]. Furthermore, the available evidence points to the fact that variations in the regional soil water are the primary driver of these strong changes in China's subtropical forests [34]. Therefore, the relationship between the different types of subtropical plantations and soil water needs to be urgently explored, as well as its main regulators. Chinese fir (*Cunninghamia lanceolata*), an important coniferous species for afforestation and timber, has been widely planted in subtropical China owing to its fast-growing and excellent timber quality [35]. The planted area of Chinese fir has reached over  $10.96 \times 10^6$  ha, accounting for 23.2% of all the plantation forests in China [36]. These Chinese fir plantations have played an essential role in timber production and soil water conservation. However, the existing Chinese fir plantations are mostly replanted monocultures, leading to a remarkably poor productivity and soil fertility [37], potentially weakening their hydrological function. Fortunately, mixed forests of Chinese fir and broadleaved tree species are proposed as an efficient way to alleviate these concerns from

different perspectives. However, the differences in soil water dynamics under different magnitudes of rainfall and their influencing factors between pure and mixed Chinese fir plantations have been rarely studied. Furthermore, whether mixed Chinese fir plantations have a positive impact on the soil water-holding capacity remains unclear. This information can provide insights into the scientific and sustainable management of subtropical forests under globally changing climate.

Stable hydrogen isotopes, as a component of water molecules, are an ideal tracer of water movement and processes [38,39]. The hydrogen isotopes in soil water can be used to characterize important hydrological processes, including the extent of soil water recharge, the different water residence time and the water flow mechanisms in the soil [40–42]. In this study, hydrogen isotopes are used to investigate the contribution of rainfall to soil water (CRSW) in a pure *C. lanceolata* plantation (PC) and two mixtures of *C. lanceolata* with *Cinnamomum camphora* (MCC) or with *Alnus cremastogyne* (MCA). Additionally, the soil properties, litter characteristics and the above- and below-ground biomasses were measured to determine the dominant factor affecting the CRSW. The aims of this study are: (i) to investigate the variation of CRSW in pure and mixed plantations of *C. lanceolata*, and (ii) to identify the determinants of the CRSW in these *C. lanceolata* plantations under different magnitudes of rainfall.

## 2. Materials and Methods

### 2.1. Site Description

The study was performed from July 2019 to December 2020, at the Huitong National Research Station of Forest Ecosystem, Chinese Academy of Sciences, Hunan Province, in China (26°51' N, 109°36' E) (Figure 1). It is located in the transition zone, from the Yunnan-Guizhou Plateau to the low hills on the southern bank of the Yangtze River, at an altitude of 300–1100 m above mean sea level. This study area has a typical subtropical humid monsoon climate with a mean annual temperature of 16.5 °C and an annual precipitation of 1200–1400 mm, of which approximately 67% occurs between April and August. The relative humidity is above 80% and the frostless season is approximately 300 days. According to the second edition of the U.S. Soil Taxonom, the soil is classified as Typic Dystrudept (sand 11.4%, silt 44.8% and clay 43.8%). The detailed data regarding the soil texture are given in Table S1. The groundwater is located at a depth of approximately 1.5–2 m below the soil surface.

The native vegetation of this region was a typical subtropical evergreen broad-leaved forest with the major species of *Castanopsis* and *Lithocarpus*. As a result of the influence of anthropogenic activities, the original zonal vegetation has almost been destroyed, and *C. lanceolata* has become the dominant forest community [43]. Furthermore, to improve the soil fertility and wood productivity of the *C. lanceolata* plantation, two broad-leaved evergreen tree species, including *Cinnamomum camphora* and *Alnus cremastogyne*, are widely used as a mixed species with Chinese fir. Specifically, *Cinnamomum camphora*, a broad-leaved evergreen tree species, is widely distributed in the subtropics. *Alnus cremastogyne* is a typical non-legume nitrogen-fixing species and a companion species for Chinese fir. To investigate the long-term effects of the different land use patterns on the evolution of the soil quality and nutrient cycling, a pure *C. lanceolata* plantation and two mixed stands of *C. lanceolata* with either *Cinnamomum camphora* or *Alnus cremastogyne* were established in the early spring of 1990, after clear-cutting a first-generation Chinese fir forest in the autumn of 1989. The ratio of Chinese fir to broad-leaved trees was 8:2. Each plantation is approximately 2.5 ha and has a planting density of 2000 stems ha<sup>-1</sup>. The three plantations at a similar altitude (495–550 m) were close to each other (26°50'56"–26°51'07" N, 109°36'08"–109°36'24" E) and had similar soil attributes before establishment [43]. These plantations also had the same southwestern exposure and a middle slope position with the slope grades of 24–26°. During the entire experiment, there was no human interference, except for that during the investigation and sampling.

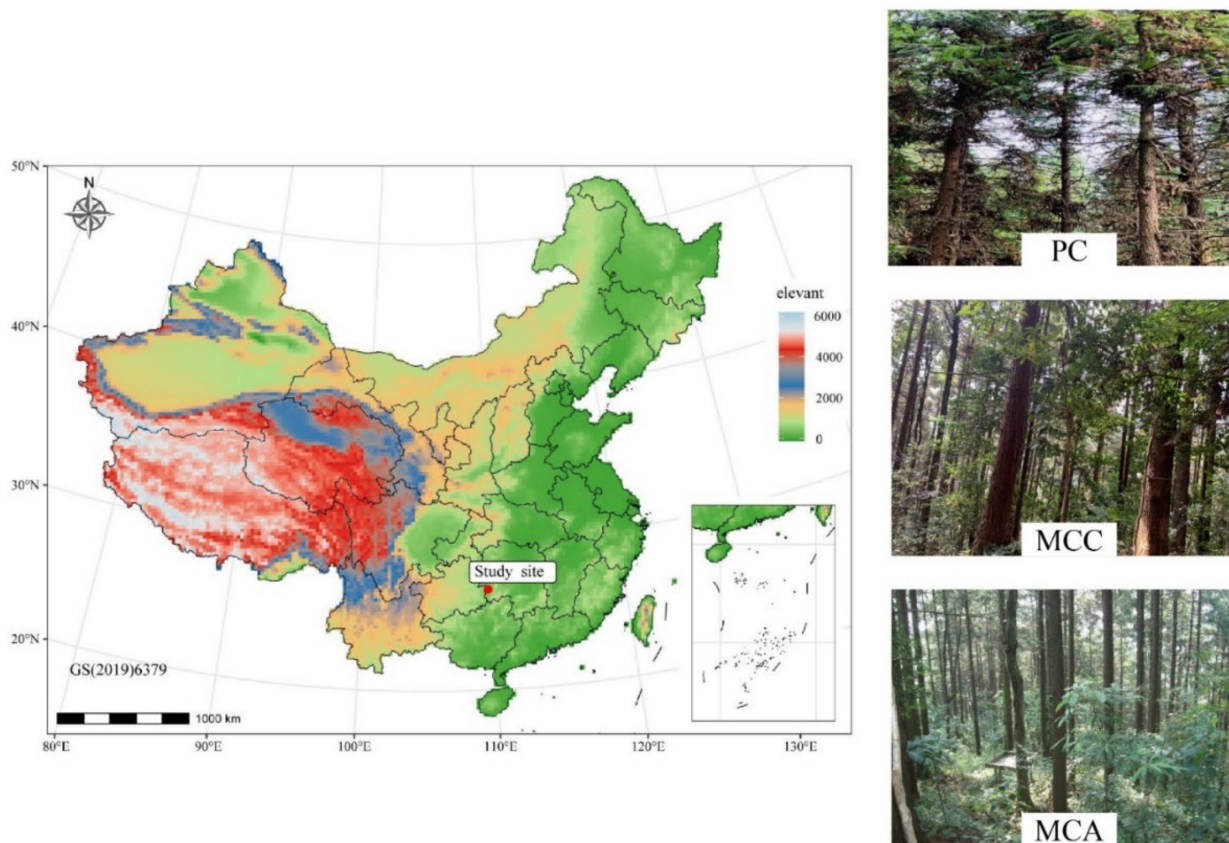


**Figure 1.** The geographical location of the study site and the landscape of different Chinese fir plantations. PC: pure *C. lanceolata* plantation; MCC: mixed plantation with *C. lanceolata* and *C. camphora*; MCA: mixed plantation with *C. lanceolata* and *A. cremastogyne*.

## 2.2. Rainfall Event Selection and Sample Collection

Based on the meteorological standards of light (0–10 mm/24 h), moderate (10–25 mm/24 h) and heavy rainfall (>25 mm/24 h), three rainfall events were selected as the experimental objects during the sampling period (15.5 mm on 18 September 2019; 36.9 mm on 26 September 2019 and 8.5 mm on 1 August 2020). In this study, we collected rainwater, shallow groundwater and soil water samples after each rainfall event until the next rainfall occurred. In addition, the soil samples were collected before each rainfall event as pre-rainfall controls. To collect the soil water samples, three 20 m × 20 m plots were randomly set up in each plantation, separated by more than 20 m and away from the boundary of each plantation. The selected plots in each plantation were visually homogeneous in structure and composition, and were dispersed over large areas to minimize spatial autocorrelation. Soil water samples were collected at each plot using a soil drill at the depths of 0–20 cm, 20–40 cm, 40–60 cm, 60–80 cm and 80–100 cm, respectively, once a day for the first 3 days after precipitation, and then every other day. Along with the soil water samples, the soil samples were collected for the determination of the soil water content (SWC, %), which was measured via oven drying at 105 °C for 24 h. To collect the rainwater samples, three rain gauge cylinders with built-in funnels were randomly placed at meteorological stations near the three plantations. A table tennis ball was placed in the funnel to avoid evaporation, which can lead to isotope fractionation [44]. The samples collected in the three rain gauge cylinders after each precipitation event were mixed and considered as one rainwater sample. The shallow groundwater near the three plantations was sampled every six days. All the collected isotope samples were immediately put into 4 mL glass vials, quickly tightened with caps, sealed with Parafilm and stored in a portable cooler at −5 to 0 °C in the field.

Following the sampling, these samples were taken back to the lab and immediately stored in the refrigerator at  $-18\text{ }^{\circ}\text{C}$  until isotopic analysis [45].

### 2.3. Sample Preparation and Stable Isotope Analysis

Firstly, we extracted the water from the soil water samples using a cryogenic vacuum distillation system [46], and the entire extraction process lasted for 1.5–3 h, depending on the sample water content. Then, the hydrogen isotope ratios of the extracted rainwater, shallow groundwater and soil water were measured using a Delta V Advantage isotope ratio mass spectrometer coupled with a Flash 2000 HT elemental analyzer (Thermo Fisher Scientific, Inc., Waltham, MA, USA) at the joint stable isotope laboratory of Shenzhen Huake Precision Analysis, Inc. (Guangdong, China) and Tsinghua Shenzhen international graduate School. The measurement accuracy for  $\delta\text{D}$  was  $\pm 1\text{‰}$ , based on three internal working standards after calibration with the Vienna Standard Mean Ocean Water standards (V-SMOW). The hydrogen isotope ratio was expressed in standard delta notion ( $\delta$ ) in parts per thousand (‰) using Equation (1):

$$\delta\text{D} = [(R_{\text{sample}}/R_{\text{standard}}) - 1] \times 1000\text{‰} \quad (1)$$

where  $R_{\text{sample}}$  and  $R_{\text{standard}}$  represent the D/H molar ratios of the water sample and the standard (V-SMOW), respectively.

### 2.4. Contribution of Rainfall to Soil Water

The source of soil water was ascertained by comparing the  $\delta\text{D}$  value of the soil water with all potential water  $\delta\text{D}$  values [45]. A two-end linear mixing model can be used to estimate the contribution of each source to soil water, if it is determined that the soil water comes from two sources [47]. Here, we found that the rainwater and shallow groundwater were the two primary sources of soil water. Therefore, the CRSW was calculated according to Equations (2)–(4):

$$\delta\text{D}_{\text{SW}} = f_{\text{R}} \times \delta\text{D}_{\text{R}} + (1 - f_{\text{R}}) \times \delta\text{D}_{\text{SG}} \quad (2)$$

$$f_{\text{R}} = (\delta\text{D}_{\text{SW}} - \delta\text{D}_{\text{SG}}) / (\delta\text{D}_{\text{R}} - \delta\text{D}_{\text{SG}}) \quad (3)$$

$$\text{CRSW} = f_{\text{R}} \times 100\% \quad (4)$$

where  $f_{\text{R}}$  is the proportion of rainfall to soil water, and  $\delta\text{D}_{\text{R}}$ ,  $\delta\text{D}_{\text{SW}}$  and  $\delta\text{D}_{\text{SG}}$  represent  $\delta\text{D}$  of the rainwater, soil water and shallow groundwater, respectively. The contribution of the rainwater to soil water was solved by Equations (2)–(4).

### 2.5. Measurement of the Vegetation and Soil Parameters

To determine the influence of the biotic and abiotic factors on the CRSW, we measured the above-ground vegetation biomass (trees, shrubs, and herbs), the litter characteristics, root biomass, and the soil properties in the three plantations. The specific methods used are as follows. For the tree above-ground biomass, first, the diameter at a breast height of 1.3 m and the tree height of all trees were measured in each plot. Then, we used the allometric growth model of *C. lanceolata* and both broad-leaved species to calculate the above-ground biomass of each tree. The total above-ground tree biomass in each plot was obtained by summing the biomass of all the trees in each plot. For the shrub biomass, all the standing shrubs within five  $5\text{ m} \times 5\text{ m}$  quadrats randomly established in each plot were investigated for their basal diameter and top height. The shrub layer biomass was calculated using a mixed model for understory shrubs provided by Huitong National Research Station of Forest Ecosystem. Herbaceous and litter biomass samples were collected in  $1\text{ m} \times 1\text{ m}$  quadrats assigned at the four corners and central point of each plot. Both herb and litter biomass samples were oven-dried to a constant weight and weighed in the laboratory. We also measured the effective water-holding capacity (EHC) and maximum water absorption rate (MWAR) of the litter using the indoor immersion method [48]. The root biomass was collected from soil depth of 0–100 cm and every 20 intervals within the  $1\text{ m} \times 1\text{ m}$  quadrats. Then, the root biomass was oven-dried to constant weight and weighed in the laboratory.

We also measured the soil properties (i.e., bulk density, total porosity and field capacity) of the three Chinese fir plantations. The soil samples were collected at the same soil depth intervals of 0–20 cm, 20–40 cm, 40–60 cm, 60–80 cm and 80–100 cm, using a stainless-steel cylindrical ring of 100 cm<sup>3</sup> volume. The above soil samples were oven-dried at 105 °C until constant weight. The bulk density (BD) was calculated using the ratio of the oven-dried soil mass to the volume of stainless-steel cylindrical ring. In addition, the total porosity (TP) and field holding capacity (FC) of all five soil layers were determined by a cutting ring method [49]. Briefly, the containers (stainless-steel cylindrical ring) with the undisturbed soil were immersed in water for 12 h, placed in a flat-bottomed tray covered with coarse dry sand for 72 h to drain excess water from the soil and then oven-dried at 105 °C to constant weight. The total porosity and field capacity were calculated according to the “Observation Methodology for Long-term Forest Ecosystem Research” of National Standards of the People’s Republic of China (GB/T 33027–2016).

### 2.6. Data Analysis

Differences in the CRSW, above-ground vegetation biomass, litter characteristics, root biomass and soil properties among the three plantations were statistically tested using one-way ANOVA and Duncan’s multiple comparison procedure, using SPSS 20.0 software (SPSS Inc., Armonk, NY, USA). An independent *t*-test was conducted to examine the differences in the soil water  $\delta D$  values between the pre- and post-rainfall samples. Significant differences were identified at a level of  $p < 0.05$ . Correlation analysis was also conducted to explore the relationship of the biotic and abiotic factors with the CRSW. To avoid autocorrelation among the indicators of the above-ground vegetation biomass, litter and soil properties, we established multivariate functional indices to represent each explanatory group using principal component analysis (PCA). The first principal component of the above-ground biomass (PC-AGB), litter properties (PC-LP) and soil properties (PC-SP) explained 85.69%, 90.61% and 72.72% of the total variation, respectively. Finally, we conducted structural equation modeling (SEM) to estimate the relative contribution, as well as the direct and indirect pathways of the abiotic and biotic factors in regulating the CRSW (Figure S1). The root biomass and the first principal component of the above-ground vegetation biomass, litter properties and soil properties were used as new variables for the SEM analysis. The following criteria were used to assess the model fit: *p*-value ( $p > 0.05$ ), chi-square tests ( $\chi^2$ ), comparative fit index (CFI) and goodness of fit index (GFI). SEM analysis was performed using the AMOS 21.0 software.

## 3. Results

### 3.1. Temporal Variation in the Soil Water Content after Different Rainfall Events

The SWC for both the monoculture and mixed plantations varied with sampling time and with the rainfall events. Following light rainfall (8.5 mm), the SWC of 0–40 cm soil layers in the 3 plantations increased and then returned to the pre-rainfall level within 5 days after the rainfall (Figure 2a–c). In contrast, the SWC in the 40–100 cm soil layers was relatively stable. Following moderate (15.5 mm) and heavy (36.9 mm) rainfall, the SWC of all soil layers showed distinct changes and exhibited an increasing trend on the first day and then gradually decreased over 7 or 11 days after rainfall (Figure 2d–i). Compared to the deep soil layers, the SWC of the shallow soil layers (0–40 cm) in the three plantations was highly variable during the sampling periods (Figure 2).

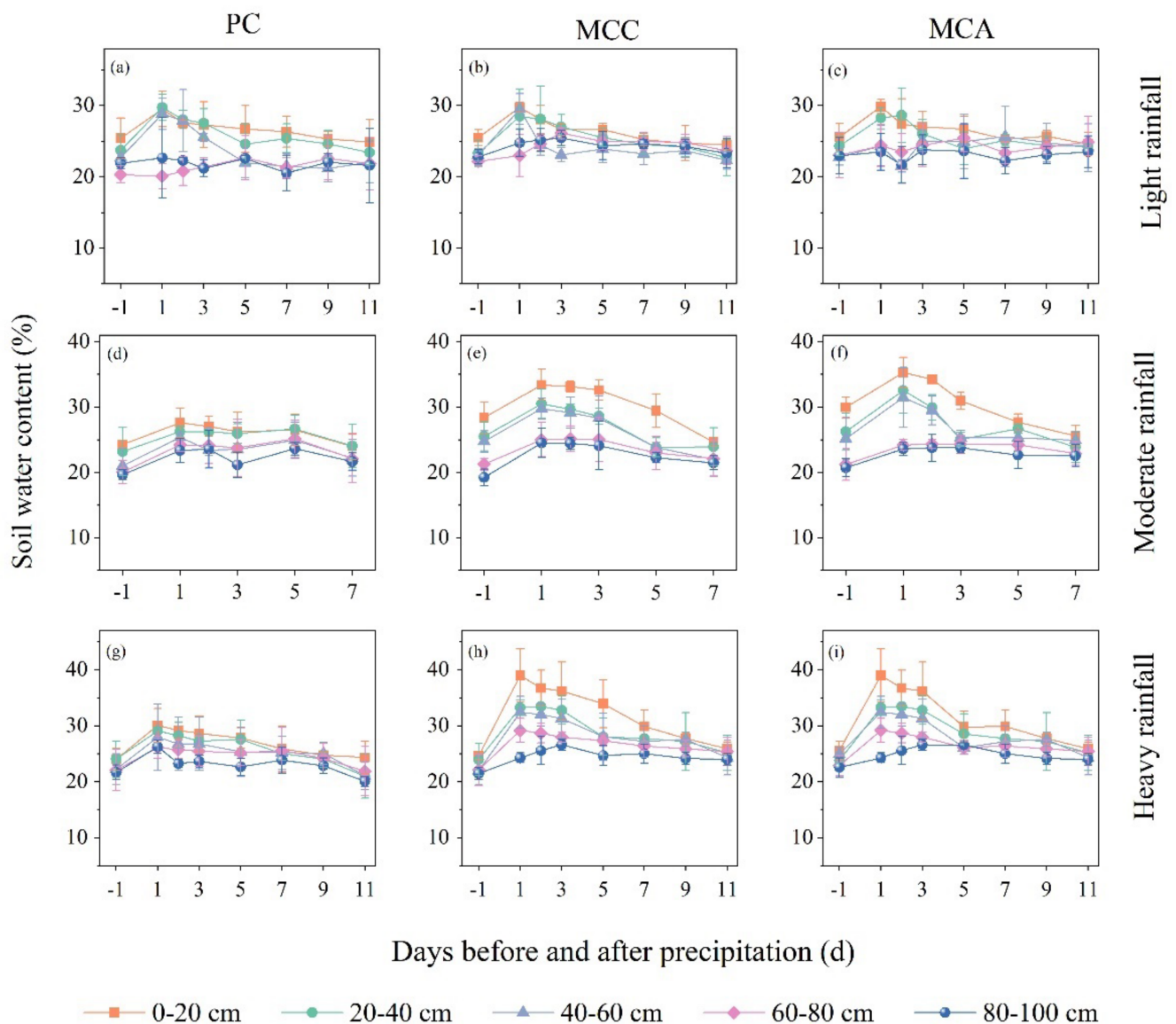


**Figure 2.** Daily soil water content (SWC) of each soil profile in PC (a,d,g), MCC (b,e,h), and MCA (c,f,i). PC: pure *C. lanceolata* plantation; MCC: mixed plantation with *C. lanceolata* and *C. camphora* and MCA: mixed plantation with *C. lanceolata* and *A. cremastogyne*.

### 3.2. Temporal Variation in the Soil Water $\delta D$ after Different Rainfall Events

During 7 or 11 days after the 3 rainfall events, the  $\delta D$  value of the soil water in PC, MCC and MCA fell between the  $\delta D$  values of rainfall and shallow groundwater (Figure 3), indicating that the soil water in these three Chinese fir stands was mainly derived from rainwater and shallow groundwater. Following light rainfall (8.5 mm), the  $\delta D$  value of the soil water in the 0–40 cm layer of PC and MCC and the 0–60 cm layer of MCA, significantly decreased on the first day, and then gradually increased during the 11 days after rainfall (Figure 3a–c and Table S2), indicating that light rainfall can infiltrate into the 0–40 cm soil layers in PC and MCC and 0–60 cm soil layers in MCA. Following moderate (15.5 mm) and heavy (36.9 mm) rainfall, the  $\delta D$  value of soil water in all layers significantly decreased on the first day and then gradually increased during 7 or 11 days after the rainfall (Figure 3d–i and Table S2).

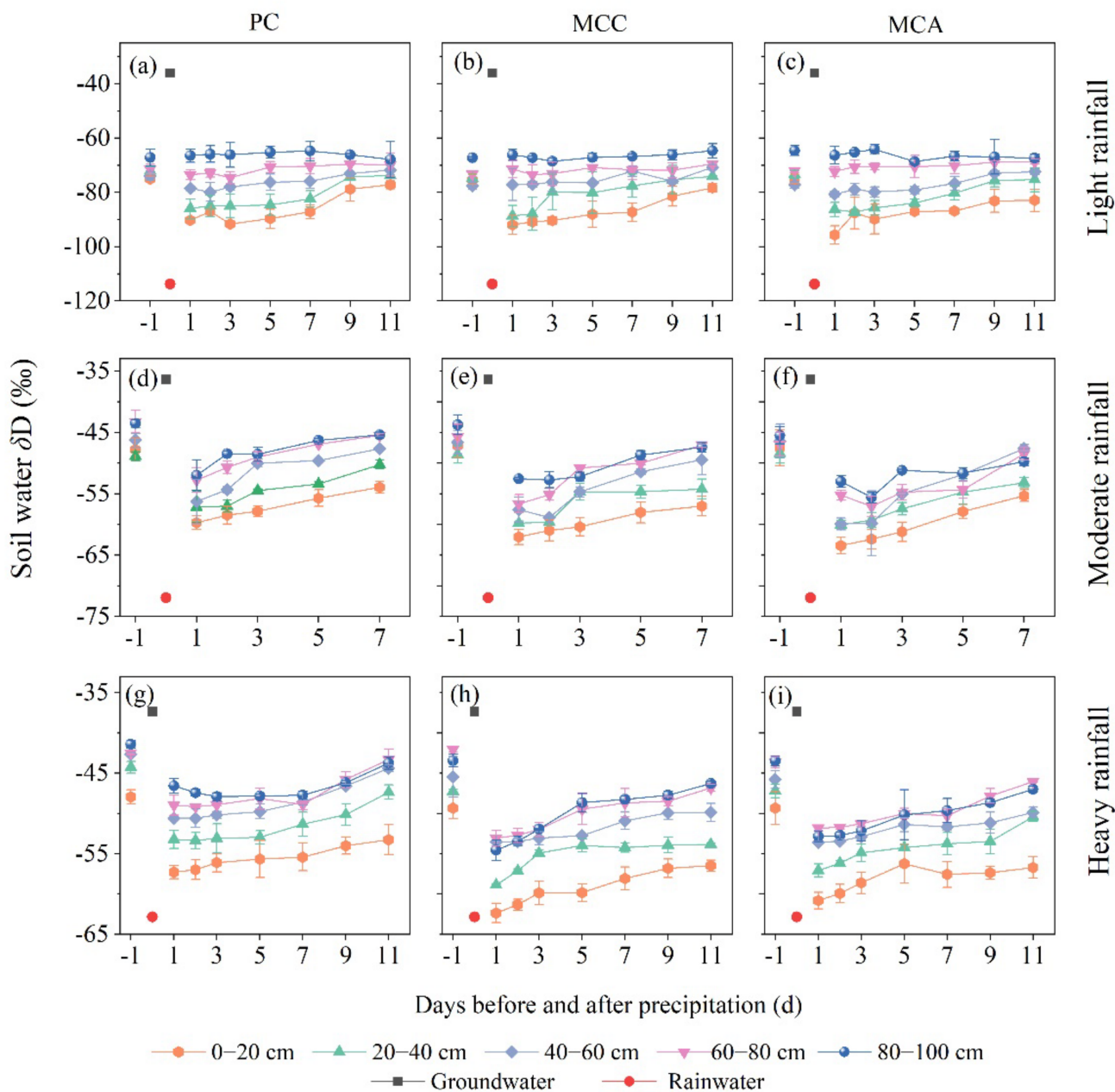


**Figure 3.** Daily  $\delta D$  of rainwater, shallow groundwater and soil water in the soil profile in PC (a,d,g), MCC (b,e,h), and MCA (c,f,i). PC: pure *C. lanceolata* plantation; MCC: mixed plantation with *C. lanceolata* and *C. camphora* and MCA: mixed plantation with *C. lanceolata* and *A. cremastogyne*.

### 3.3. Variation of CRSW among the Three Plantations

Following the light rainfall event, there was no significant difference in the CRSW at all depths among the three plantations (Figure 4a–e and Table S3). In general, the contribution of moderate rainfall to the soil water (CMRSW) was higher in MCC and MCA than in PC at all depths (average: 44.07%, 51.10% and 54.06%, respectively), although significant differences were only found at the depths of 0–20 cm and 60–100 cm (Figure 4f–j and Table S3). Similarly, following the heavy rainfall event, the CRSW of MCC and MCA at all depths was significantly higher than that of PC (average: 62.74%, 61.18% and 49.77%, respectively), whereas there was no difference among those of MCC and MCA (Figure 4f–j and Table S3).

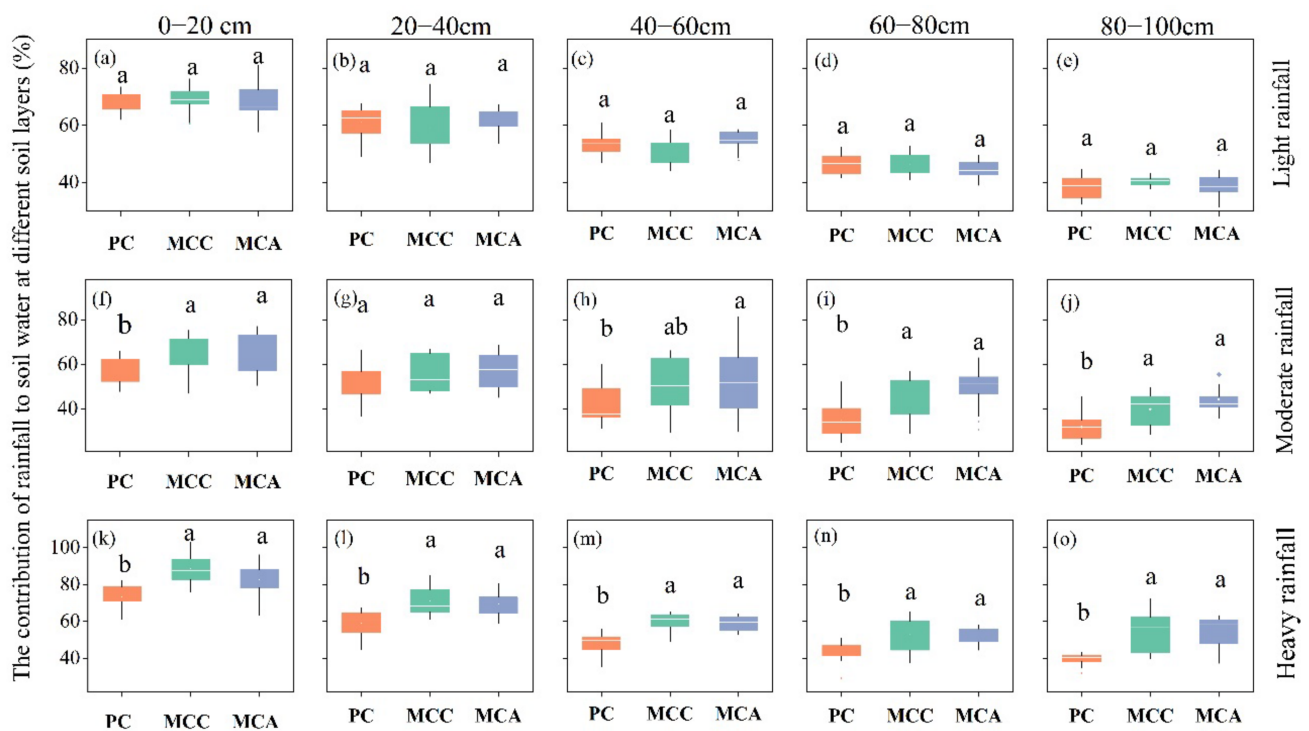


**Figure 4.** Comparison of the contribution of light (a–e), moderate (f–j) and heavy (k–o) rainfall to soil water among the three plantations. PC: pure *C. lanceolata* plantation; MCC: mixed plantation with *C. lanceolata* and *C. camphora* and MCA: mixed plantation with *C. lanceolata* and *A. cremastogyne*. The different lowercase letters indicate significant differences among the three plantations ( $p < 0.05$ ).

### 3.4. The Correlation of Vegetation Biomass, Litter Characteristics, Root Biomass and Soil Properties with the CRSW

The correlation analysis results shows that both the root biomass and PC-SP are positively correlated with the CRSW following the three rainfall events ( $p < 0.001$ , Figure 5). The PC-LP does not have a significant correlation with the CRSW after light rainfall, while it shows a positive correlation with CRSW after moderate and heavy rainfall ( $p < 0.01$ , Figure 5). After light rainfall, there is no significant correlation between PC-AGB and CRSW (Figure 5). After moderate rainfall, the PC-AGB is positively correlated with the CRSW ( $p < 0.05$ , Figure 5). Similarly, the PC-AGB has a positive correlation with the CRSW after heavy rainfall ( $p < 0.01$ , Figure 5). These results suggest that both the vegetation and soil properties can affect the CRSW under different magnitude rainfall events.

To elucidate the reasons for the differences in CRSW among the three Chinese fir plantations, the differences in the vegetation and soil properties of these plantations were compared (Tables 1 and 2). The tree biomass, shrub biomass and total root biomass of MCC and MCA were significantly higher than those of the PC ( $p < 0.05$ , Table 1). Similarly, the litter mass, EHC and MWAR were significantly greater in MCC and MCA than those in the PC ( $p < 0.05$ , Table 1). The herb biomass had a trend of PC < MCA < MCC (Table 1). Additionally, the root biomass in MCC and MCA was higher than that in the PC, except in the 40–80 cm soil layer (Table 2). Compared with those of the PC, the MCC and MCA showed a significantly lower bulk density at all depths ( $p < 0.05$ , Table 2), and a significantly greater field capacity and total porosity, except in the 60–80 cm layer (Table 2). There was no significant difference between most of these variables for MCC and MCA (Table 2).

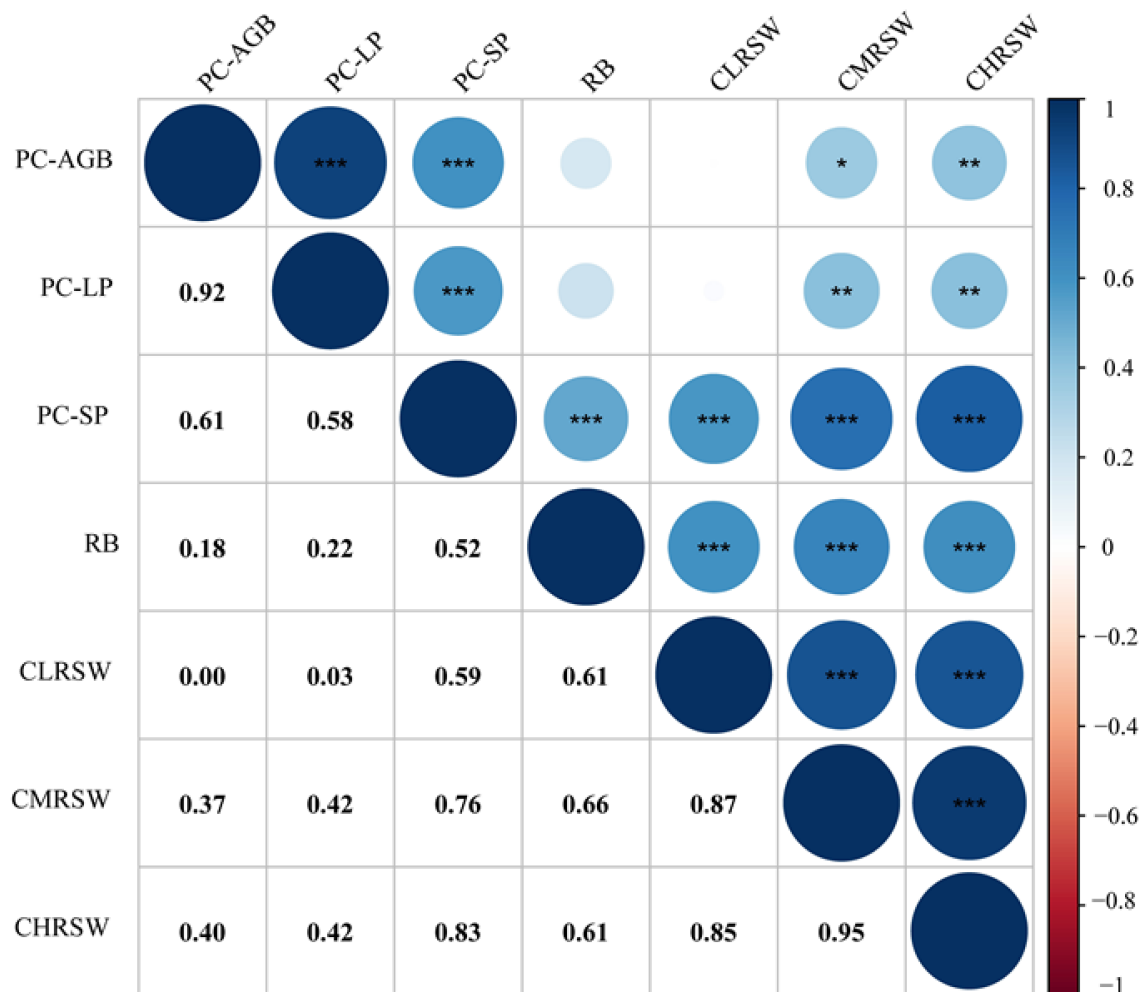


**Figure 5.** Correlation analysis of the CRSW with the vegetation and soil properties under the three rainfall events. PC-AGB: the first component from the principal components analysis of the above-ground biomass (TB, SB and HB); PC-LP: the first component from the principal components analysis of the litter properties (LM, EHC and MWAR); PC-SP: the first component from the principal components analysis of the soil properties (BD, TP and FC); RB: root biomass; CLRSW: the contribution of light rainfall to soil water; CMRSW: the contribution of moderate rainfall to soil water and CHRWSW: the contribution of heavy rainfall to soil water; \*  $p < 0.05$ , \*\*  $p < 0.01$ , \*\*\*  $p < 0.001$ .

**Table 1.** The vegetation and litter characteristics among the three plantations.

Vegetation and Litter Characteristics	Variable	PC	MCC	MCA
Above-ground biomass	Tree biomass ( $\text{kg}\cdot\text{m}^{-2}$ )	$10.34 \pm 1.69$ b	$20.14 \pm 0.93$ a	$22.46 \pm 1.00$ a
	Shrub biomass ( $\text{g}\cdot\text{m}^{-2}$ )	$2.68 \pm 0.02$ b	$12.54 \pm 2.12$ a	$10.93 \pm 0.84$ a
	Herb biomass ( $\text{g}\cdot\text{m}^{-2}$ )	$269.31 \pm 6.43$ b	$399.35 \pm 46.22$ a	$319.40 \pm 8.54$ b
Litter characteristics	Litter mass ( $\text{t}\cdot\text{hm}^{-2}$ )	$7.94 \pm 0.22$ b	$8.83 \pm 0.17$ a	$8.88 \pm 0.53$ a
	EHC ( $\text{t}\cdot\text{hm}^{-2}$ )	$12.62 \pm 1.44$ b	$17.94 \pm 0.97$ a	$17.62 \pm 2.26$ a
	MWAR ( $\text{g}\cdot\text{kg}^{-1}\cdot\text{h}^{-1}$ )	$81.44 \pm 7.31$ b	$100.27 \pm 4.52$ a	$97.47 \pm 10.65$ a

The results are reported as means  $\pm$  SD. The different lowercase letters in the same row indicate the significant differences at a 0.05 probability level. PC: pure *C. lanceolata* plantation; MCC: mixed plantation with *C. lanceolata* and *C. camphora*; MCA: mixed plantation with *C. lanceolata* and *A. cremastogyne*; EHC: effective holding capacity and MWAR: maximum water absorption rate.

**Table 2.** The soil properties and root biomass among the three plantations.

Variable	Layers (cm)	PC	MCC	MCA
Bulk density (g·m <sup>-3</sup> )	0–20	1.31 ± 0.02 a	1.25 ± 0.02 b	1.24 ± 0.03 b
	20–40	1.36 ± 0.01 a	1.33 ± 0.02 b	1.33 ± 0.01 b
	40–60	1.42 ± 0.03 a	1.34 ± 0.02 b	1.34 ± 0.04 b
	60–80	1.46 ± 0.02 a	1.41 ± 0.05 b	1.40 ± 0.05 a
	80–100	1.46 ± 0.01 a	1.42 ± 0.03 ab	1.42 ± 0.06 b
Field capacity (%)	0–20	35.01 ± 0.99 b	41.48 ± 1.19 a	40.69 ± 3.61 a
	20–40	28.75 ± 1.34 c	38.23 ± 0.56 a	35.10 ± 1.37 b
	40–60	27.88 ± 1.91 b	42.33 ± 3.65 a	31.99 ± 1.57 a
	60–80	34.49 ± 4.10 a	35.98 ± 4.61 a	31.58 ± 1.44 a
	80–100	25.27 ± 3.50 b	32.18 ± 0.48 a	36.82 ± 3.18 a
Total porosity (%)	0–20	45.79 ± 0.60 b	50.90 ± 2.45 a	49.58 ± 1.49 a
	20–40	39.07 ± 1.82 b	48.03 ± 3.08 a	45.34 ± 2.96 a
	40–60	39.68 ± 2.50 a	46.65 ± 5.81 a	43.31 ± 1.56 a
	60–80	43.70 ± 1.00 a	46.65 ± 3.41 a	44.62 ± 0.27 a
	80–100	40.43 ± 2.44 b	46.82 ± 1.02 a	45.24 ± 1.67 a
Root biomass (g·m <sup>-2</sup> )	0–20	128.60 ± 54.43 b	136.17 ± 13.62 b	325.72 ± 58.58 a
	20–40	103.37 ± 17.94 a	157.39 ± 25.42 a	152.31 ± 44.20 a
	40–60	119.09 ± 27.26 a	96.08 ± 51.56 a	96.19 ± 4.79 a
	60–80	111.08 ± 37.92 a	90.07 ± 48.65 a	133.11 ± 67.48 a
	80–100	29.74 ± 19.45 b	30.93 ± 3.76 b	110.78 ± 9.81 a
	Total	491.87 ± 53.87 b	510.63 ± 128.25 b	818.11 ± 124.80 a

The results are reported as means ± SD. The different lowercase letters in the same row indicate significant differences at a 0.05 probability level. PC: pure *C. lanceolata* plantation; MCC: mixed plantation with *C. lanceolata* and *C. camphora*; MCA: mixed plantation with *C. lanceolata* and *A. cremastogyne*; EHC: effective holding capacity and MWAR: maximum water absorption rate.

### 3.5. The Factors Affecting the CRSW under Different Rainfall Events

To further determine the direct and indirect effects of the above biotic and abiotic factors on the CRSW and to quantify their relative importance, we constructed three structural equation models based on the correlation results between each factor with the CRSW. As shown by the SEM analysis, these three models, including all the parameters, showed good fit criteria and explained 63–73% of the variance in the CRSW (Figure 6). During the light rainfall event, the soil properties and root biomass had a direct and positive effect on the CRSW with the path coefficients of 0.69 and 0.32, respectively. In contrast, the above-ground vegetation biomass had a direct and negative effect on the CRSW (path coefficient = −0.48) (Figures 6a and 7a). During the moderate and heavy rainfall events, the soil properties exerted the strongest direct positive effect on the CRSW (path coefficients = 0.61 and 0.76), and the root biomass had a direct positive effect on it (path coefficients = 0.36 and 0.23), while the above-ground vegetation biomass had an insignificant negative effect on the CRSW (Figures 6b,c and 7b,c). Moreover, the above-ground vegetation biomass showed an indirect effect on the CRSW under the three rainfall events because of its positive impact on litter properties. Similarly, the root biomass and litter properties indirectly affected the CRSW through the soil properties.

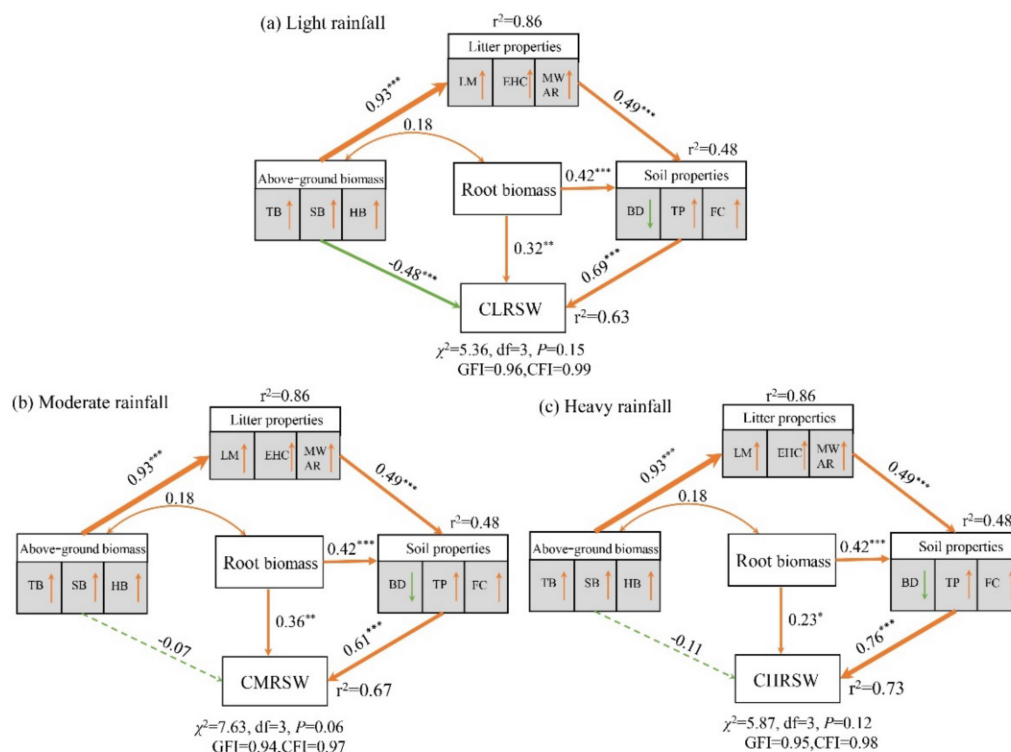


**Figure 6.** Structural equation models showing the multivariate effects on the contribution of rainfall to soil water. The double-layered rectangle represents the first principal component of the principal component analysis (PCA) for above-ground biomass, litter and soil properties. Above-ground biomass includes TB (tree biomass), SB (shrub biomass) and HB (herb biomass). Litter properties include LM (litter mass), EHC (Effective holding capacity) and MWAR (maximum water absorption rate). Soil properties include BD (bulk density), TP (total porosity) and FC (field capacity). CLRSW: the contribution of light rainfall to soil water; CMRSW: the contribution of moderate rainfall to soil water and CHRSW: the contribution of heavy rainfall to soil water. The numbers on the arrows are the standardized path coefficients. The larger path coefficients are reflected by the width of the arrow, with the orange solid lines indicating a significantly positive effect, the green solid lines indicating a significantly negative effect and the blue dashed lines indicating that the effect was not significant. The goodness-of-fit statistics of the model are displayed below the model. \*  $p < 0.05$ , \*\*  $p < 0.01$ , \*\*\*  $p < 0.001$ .

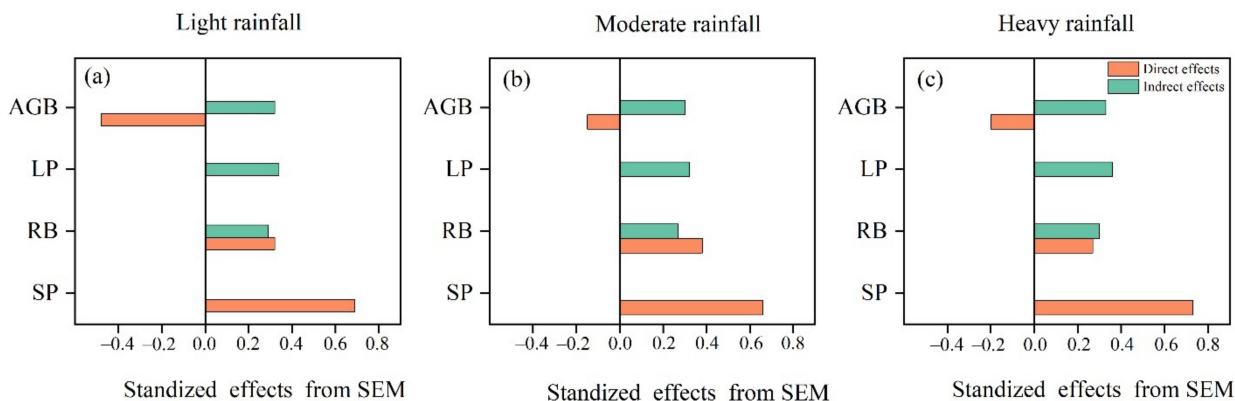


**Figure 7.** Standardized effects on the CRSW derived from the structural equation modeling (SEM). The orange and green bars represent the direct and indirect effects of various factors on the contribution of (a) light rainfall, (b) moderate rainfall and (c) heavy rainfall to soil water from SEM. AGB: above-ground biomass; LP: litter properties; SP: soil properties and RB: root biomass.

## 4. Discussion

### 4.1. The Response of the SWC and Soil Water $\delta D$ to Rainfall Events

The response of the SWC and soil water  $\delta D$  values in the vertical profiles varied with the rainfall events in Chinese fir plantations (Figures 2 and 3). The fluctuation in the SWC and soil water  $\delta D$  values merely occurred in shallow soil layers (0–40 cm), following the light rainfall event. However, with the increase in precipitation, the SWC and soil water  $\delta D$  values fluctuated more obviously because of the input of vast amounts of rainwater and the higher soil connectivity, which allowed more water to infiltrate the deep soil layers [24]. Hence, the SWC and soil water  $\delta D$  values were significantly influenced in the entire 0–100 cm layer after heavy rainfall. This observation suggests that the wetting front caused by the heavy rainfall on these stands extended down to approximately 100 cm [50], facilitating the utilization of soil water by deep-rooted plants and the recharge of groundwater [51]. In addition, after three rainfall events, the  $\delta D$  value of the surface soil water was lower than that of the deeper soil layers (Figure 3). This might be related to the input of rainfall with a negative  $\delta D$  value, demonstrating the strong effect of precipitation at shaping the isotopic composition of soil water [38,39]. Meanwhile, we found that the SWC and soil water  $\delta D$  of shallow layers showed the highest variations among 0–100 cm soil layers after the 3 rainfall events. This was consistent with the results of a previous study, indicating that the combined influence of evaporation and precipitation resulted in a high variability of the topsoil water [52].

### 4.2. The Variation in the CRSW in Different Plantations and Its Direct Regulators

In this study, we did not observe significant differences in the contribution of light rainfall to soil water (CLRSW) between pure and mixed plantations. This phenomenon was possibly because of the variations in the ability of vegetation and soil to intercept and retain light rainfall in different plantation types (Figures 6a and 7a). Vegetation and soil are the first and second active layers of rainfall partitioning in forest ecosystems [53,54]. The biomass-related indicators (i.e., leaf biomass and woody biomass) and soil properties (i.e., bulk density and total porosity) exhibited a significant linear relationship with the interception capacity for light rainfall events [12,55]. Therefore, compared with MCC and MCA, the smaller above-ground biomass of pure Chinese fir can decrease the ability of vegetation to intercept rainfall, thereby increasing the proportion of rainfall allocated to the soil. However, among the three stands, the PC had the highest bulk density and lowest total porosity, which can reduce the amount of pore space in the soil, and slow the downward flow of rainfall, resulting in a lower infiltration rate of precipitation and weakening the interception of precipitation by the soil [25,56,57], possibly even causing part of the light rainfall to be lost through evaporation during infiltration. This adverse effect of the soil properties in PC on the CLRSW, counteracted or masked the positive effect of the smaller above-ground biomass to a certain extent. By contrast, the lower bulk density and higher total porosity in MCC and MCA were conducive to intercepting and retaining the rainfall, despite the relatively greater interception induced by the higher above-ground biomass relative to that in the PC. Moreover, vegetation root systems dominate the hydrological processes at the root–soil interface. The root biomass in the two mixed plantations was greater than that in pure Chinese fir plantation, which could increase the air entry value and the size of the hysteresis loop, inducing high suction [58,59], and thus helping the soil of the mixed plantations to retain more precipitation. Overall, the offsetting effects of the vegetation and soil properties together regulated the soil water dynamics under light rainfall and drove non-difference in CLRSW among the three Chinese fir plantations.

The higher CRSW observed in MCC and MCA, in comparison with that in PC after moderate and heavy rainfall events, demonstrated the higher capacity of the mixed species plantations to intercept and retain moderate and heavy rainfall. The above-ground biomass was no longer the limiting factor influencing the CRSW following moderate and heavy rainfall events, as expressed by the SEM, as vegetation interception only accounts for a small fraction of the precipitation when the rainfall is heavy [60], causing most rainfall to infiltrate

the soil. Our results demonstrated that soil the properties were the dominant direct factor controlling CRSW under moderate and heavy rainfall events (Figures 6b,c and 7b,c). This is consistent with the findings of previous studies [28], suggesting the vital role of soil properties in intercepting and retaining rainfall, especially in the case of heavy precipitation. It has been suggested that soil properties (i.e., bulk density, soil porosity or field capacity) were closely related to the soil hydraulic conductivity and determined the soil water-holding capacity [10,20,24]. We found that the bulk density had the strongest correlation with the CRSW (Table S4), as bulk density is closely related to soil texture structure, and a reduction in its value enhances soil porosity, aeration and permeability [61]. Moreover, the total porosity and field capacity were also important driving factors, both showing a significantly positive correlation with the CRSW. The positive effects of the total porosity on the CRSW can be attributed to the fact that soil with high total porosity can provide more effective space for rainwater infiltration, thus enhancing the stand capacity for intercepting precipitation [62]. The interaction between bulk density and porosity (i.e., macropores) can also promote soil water infiltration [63]. Finally, the field capacity itself represents the maximum soil water-holding capacity under adequate precipitation conditions. These results implied that favorable soil conditions, accompanied by a low bulk density, a high total porosity and field capacity can enhance infiltration and the water-holding capacity. Therefore, compared to monoculture, both mixed plantations had significantly better soil properties, leading to an increased ability to intercept and retain moderate and heavy rainfall. Additionally, mixed species plantations with complex stand structures and high species richness and diversity, can decrease water evaporation through spatial structure-related shading effects and/or reduce soil erosion, which helps maintain and increase soil water [64,65].

#### 4.3. Key Indirect Regulators of the CRSW

The hydrological functions of the root system have been underestimated or even neglected in many previous studies [51]. However, our results show that root biomass has a bidirectional effect on the CRSW (Figures 6 and 7). The continuous pore network formed by plant roots is an important channel for water infiltration in soil. Huang (2016) indicated that the soil infiltration capacity was positively related to below-ground biomass [66]. Hence, the higher root biomass in the two mixed plantations than that in the pure Chinese fir plantation could have allowed more rainwater to infiltrate the soil, thus resulting in a better ability to intercept moderate and heavy rainfall. More importantly, the root biomass indirectly and positively affected the CRSW by modifying the soil properties, possibly via two aspects. First, the plant roots can improve the soil structural stability by enmeshing and realigning soil particles and releasing exudates, thus affecting the soil permeability and erosion resistance [67,68]. Second, the processes of the growth, death and decomposition of roots can increase the soil organic matters and form soil pores, thereby promoting soil porosity and reducing bulk density [69,70], which determined the soil capacity for infiltration and precipitation interception. Indeed, the broad-leaved trees in the two mixed Chinese fir plantations increased the soil organic concentrations by allocating more biomass to the root systems [35], thus improving their ability to intercept rainwater. In our study, the soil organic carbon concentrations in the mixed plantations were higher than those in the pure Chinese fir plantation, further confirming the above inference (Table S5). Meanwhile, the increase in the root biomass can pose positive impacts of soil properties on the CRSW after rainfall [28]. Taken together, the lowest root biomass observed for the PC, when comparing all plantations, weakened the soil's ability to intercept and retain rainfall.

In addition to root biomass, litter can also influence the soil water-holding capacity by altering the soil properties (Figures 6 and 7). Litter is a major source of soil carbon and its decomposition helps regulate nutrient cycling and soil fertility. The increased input of broad-leaved and herbaceous biomass in the two mixed plantations contributed to mediating soil biological activity, accelerating litter decomposition and increasing the soil carbon level [43,71,72]. These changes in soil properties can improve the soil aggregate

stability and porosity, and reduce the bulk density [73], ultimately improving the soil water-holding capacity. In addition, mixed species stands can enhance the soil hydraulic conductivity by increasing the buffering and interception capacity of the litter layer [74,75], thus improving the CRSW. The significantly higher litter mass and effective water-holding capacity in MCC and MCA compared with those in PC, suggest that the two mixed plantations can intercept more rainfall, thereby increasing the soil water flux [76]. Therefore, the quality and quantity of litter in MCC and MCA improved the soil water-holding capacity compared to PC.

## 5. Conclusions

The results of this study demonstrate that mixed Chinese fir plantations exhibit a higher capacity to intercept and retain rainfall than monospecific plantations during moderate and heavy rainfall events. The higher capacity of mixed plantations was tightly and directly associated with improved soil properties, and indirectly related to root biomass and litter characteristics. Furthermore, the capacity of Chinese fir plantations to intercept and retain light rainfall was regulated by both the vegetation and soil properties. These observations provide new insights into the effects of the afforestation models on hydrological functions and have the following implications: first, mixed conifer–broad-leaved forests possess a greater capacity to intercept and retain precipitation than a pure conifer forest, which is conducive to improving soil water conservation and mediating floods in humid subtropical regions. Moreover, our findings show that the main factors regulating the capacity of stands to intercept rainfall varied with the magnitude of precipitation. This result emphasizes the importance of investigating various precipitation levels in future studies attempting to explore the dominant factors affecting the capacity of stands to intercept rainfall. In addition, this study used samples collected in only one subtropical area, and there can be spatiotemporal variations in the capacity of plantations to intercept and retain precipitation under different climatic regimes. Future studies should thus consider multiple sampling sites, so that the spatiotemporal variations and interactions between soil water conservation and forest types can be elucidated in detail.

**Supplementary Materials:** The following supporting information can be downloaded at: <https://www.mdpi.com/article/10.3390/f13010123/s1>, Figure S1: A priori model of variables on the contribution of rainfall to soil water (CRSW); Table S1: Soil texture for the study site. Table S2: Results of comparing pre-rainfall and first day after rainfall of soil water  $\delta D$ . Table S3: Results of comparing the contribution of rainfall to soil water among the three plantations. Table S4: Correlation coefficient between CRSW, vegetation properties and soil properties. Table S5: Soil organic carbon concentration among the three plantations.

**Author Contributions:** Conceptualization, Y.Z. and Q.X.; methodology, Q.X.; software, Y.Z., B.Z. and R.R.; validation, Y.Z. and J.J.; formal analysis, Y.Z. and B.Z.; investigation, Y.Z., D.G. and W.X.; resources, Y.Z. and B.Z.; data curation, Y.Z. and Q.X.; writing—original draft preparation, Y.Z.; writing—review and editing, Y.Z., J.J., Q.X. and S.W.; visualization, W.X.; supervision, Q.X.; project administration, Q.X.; funding acquisition, Q.X. All authors have read and approved the final manuscript.

**Funding:** This study was supported by the National Natural Science Foundation of China (31870716; 31670720) and the National Nonprofit Institute Research Grant of CAF (CAFYBB2017ZB003; CAFYBB2021ZE002).

**Institutional Review Board Statement:** Not applicable.

**Informed Consent Statement:** Not applicable.

**Data Availability Statement:** The datasets used and/or analyzed during this study are available from the corresponding author upon reasonable request.

**Acknowledgments:** We are very grateful to the Huitong National Research Station of Forest Ecosystem for their support and assistance in the fieldwork.

**Conflicts of Interest:** The authors declare no conflict of interest.

## References

- Legates, D.R.; Mahmood, R.; Levia, D.F.; Deliberty, T.L.; Quiring, S.M.; Houser, C.; Nelson, F.E. Soil moisture: A central and unifying theme in physical geography. *Prog. Phys. Geog.* **2011**, *35*, 65–86. [[CrossRef](#)]
- Moreno-Gutierrez, C.; Dawson, T.E.; Nicolas, E.; Querejeta, J.I. Isotopes reveal contrasting water use strategies among coexisting plant species in a Mediterranean ecosystem. *New Phytol.* **2012**, *196*, 489–496. [[CrossRef](#)] [[PubMed](#)]
- Jiao, Y.; Lei, H.; Yang, D.; Huang, M.; Liu, D.; Yuan, X. Impact of vegetation dynamics on hydrological processes in a semi-arid basin by using a land surface-hydrology coupled model. *J. Hydrol.* **2017**, *551*, 116–131. [[CrossRef](#)]
- Wang, C.; Fu, B.; Zhang, L.; Xu, Z. Soil moisture-plant interactions: An ecohydrological review. *J. Soil Sediment.* **2019**, *19*, 1–9. [[CrossRef](#)]
- Jiao, L.; An, W.; Li, Z.; Gao, G.; Wang, C. Regional variation in soil water and vegetation characteristics in the Chinese Loess Plateau. *Ecol. Indic.* **2020**, *115*, 106399. [[CrossRef](#)]
- Chen, G.; Tan, Q.; Xu, M.; Liu, G. Mixed-species plantations can alleviate water stress on the Loess Plateau. *For. Ecol. Manag.* **2020**, *458*, 117767.
- Fischer, C.; Roscher, C.; Jensen, B.; Eisenhauer, N.; Baade, J.; Attinger, S.; Scheu, S.; Weisser, W.W.; Schumacher, J.; Hildebrandt, A. How do earthworms, soil texture and plant composition affect infiltration along an experimental plant diversity gradient in grassland? *PLoS ONE* **2014**, *9*, e98987. [[CrossRef](#)] [[PubMed](#)]
- Taylor, C.M.; Belusic, D.; Guichard, F.; Arker, D.; Vischel, T.; Bock, O.; Harris, P.P.; Janicot, S.; Klein, C.; Panthou, G. Frequency of extreme Sahelian storms tripled since 1982 in satellite observations. *Nature* **2017**, *544*, 475–478. [[CrossRef](#)] [[PubMed](#)]
- Myhre, G.; Samset, B.; Hodnebrog, Ø.; Andrews, T.; Boucher, O.; Faluvegi, G.; Fläschner, D.; Forster, P.M.; Kasoar, M.; Kharin, V.; et al. Sensible heat has significantly affected the global hydrological cycle over the historical period. *Nat. Commun.* **2018**, *9*, 1922. [[CrossRef](#)] [[PubMed](#)]
- Metzger, J.C.; Wutzler, T.; Valle, N.D.; Filipzik, J.; Hildebrandt, A. Vegetation impacts soil water content patterns by shaping canopy water fluxes and soil properties. *Hydrol. Process.* **2017**, *31*, 3783–3795. [[CrossRef](#)]
- Solomou, A.D.; Skoufogianni, E.; Danalatos, N.G. Exploitation of soil properties for controlling herbaceous plant communities in an organic cultivation of lippia citriodora in the mediterranean landscape. *Bulg. J. Agric. Sci.* **2020**, *26*, 7983.
- Li, X.; Xiao, Q.; Niu, J.; Dymond, S.; Doorn, N.; Yu, X.; Xie, B.; Lv, X.; Zhang, K.; Li, J. Process-based rainfall interception by small trees in Northern China: The effect of rainfall traits and crown structure characteristics. *Agric. For. Meteorol.* **2016**, *218*, 65–73. [[CrossRef](#)]
- Song, X.; Lyu, S.; Wen, X. Limitation of soil moisture on the response of transpiration to vapor pressure deficit in a subtropical coniferous plantation subjected to seasonal drought. *J. Hydrol.* **2020**, *591*, 125301. [[CrossRef](#)]
- Zhao, C.; Jia, X.; Zhu, Y.; Shao, M. Long-term temporal variations of soil water content under different vegetation types in the Loess Plateau, China. *Catena* **2017**, *158*, 55–62. [[CrossRef](#)]
- Saija, H.; Timo, D.; Leena, F.; Jarkko, H.; Juho, M.; Jari, M.; Seppo, N.; Pentti, N.; Ari, N.; Tuula, P.; et al. What is the potential for replacing monocultures with mixed-species stands to enhance ecosystem services in boreal forests in Fennoscandia? *For. Ecol. Manag.* **2021**, *479*, 118558.
- Bouwman, M.; Forrester, D.I.; Ouden, J.D.; Nabuurs, G.J.; Mohren, G. Species interactions under climate change in mixed stands of Scots pine and pedunculate oak. *For. Ecol. Manag.* **2020**, *481*, 118615. [[CrossRef](#)]
- Pretzsch, H.; Schütze, G.; Uhl, E. Resistance of European tree species to drought stress in mixed versus pure forests: Evidence of stress release by inter-specific facilitation. *Plant Biology* **2013**, *15*, 483–495. [[CrossRef](#)] [[PubMed](#)]
- Metz, J.; Annighofer, P.; Schall, P.; Zimmermann, J.; Kahl, T.; Schulze, E.D.; Ammer, C. Site-adapted admixed tree species reduce drought susceptibility of mature European beech. *Glob. Chang. Biol.* **2016**, *22*, 903–920. [[CrossRef](#)]
- Sui, M.; Zhang, B.; Xu, Q.; Gao, D.; Zhang, Y.; Wang, S. Effects of plantation types and patterns on rainfall partition in soil in a mid-subtropical region of China. *Plant Soil* **2021**, *466*, 1–15. [[CrossRef](#)]
- Primicia, I.; Camarero, J.J.; Imbert, J.B.; Castillo, F.J. Effects of thinning and canopy type on growth dynamics of *Pinus sylvestris*: Inter-annual variations and intra-annual interactions with microclimate. *Eur. J. For. Res.* **2013**, *132*, 121–135. [[CrossRef](#)]
- Niether, W.; Schneidewind, U.; Armengot, L.; Adamtey, N.; Schneider, M.; Gerold, G. Spatial-temporal soil moisture dynamics under different cocoa production systems. *Catena* **2017**, *158*, 340–349. [[CrossRef](#)]
- Sun, L.; Yang, L.; Chen, L.; Li, S.; Zhao, F.; Sun, S. Tracing the soil water response to autumn rainfall in different land uses at multi-day timescale in a subtropical zone. *Catena* **2019**, *180*, 355–364. [[CrossRef](#)]
- Li, B.; Biswas, A.; Wang, Y.; Li, Z. Identifying the dominant effects of climate and land use change on soil water balance in deep loessial vadose zone. *Agr. Water Manag.* **2020**, *245*, 106637. [[CrossRef](#)]
- Dai, L.; Yuan, Y.; Guo, X.; Du, Y.; Cao, G. Soil water retention in alpine meadows under different degradation stages on the northeastern Qinghai-Tibet Plateau. *J. Hydrol.* **2020**, *590*, 125397. [[CrossRef](#)]
- Wei, X.; Liang, W. Regulation of stand density alters forest structure and soil moisture during afforestation with *Robinia pseudoacacia* L. *Pinus tabulaeformis* Carr. On the Loess Plateau. *For. Ecol. Manag.* **2021**, *491*, 119196.

26. Korres, W.; Reichenau, T.G.; Fiener, P.; Koyama, C.N.; Bogen, H.R.; Cornelissen, T.; Baatz, R.; Herbst, V.; Dieckkrüger, B.; Vereecken, H.; et al. Spatio-temporal soil moisture patterns—A meta-analysis using plot to catchment scale data. *J. Hydrol.* **2014**, *520*, 326–341. [[CrossRef](#)]
27. Yue, K.; Frenne, P.D.; Fornara, D.A.; Meerbeek, K.V.; Li, W.; Peng, X.; Ni, X.; Peng, Y.; Wu, F.; Yang, Y.; et al. Global patterns and drivers of rainfall partitioning by trees and shrubs. *Glob. Chang. Biol.* **2021**, *27*, 3350–3357. [[CrossRef](#)] [[PubMed](#)]
28. Zhang, B.; Xu, Q.; Gao, D.; Jiang, C.; Ma, Y. Higher soil capacity of intercepting heavy rainfall in mixed stands than in pure stands in riparian forests. *Sci. Total Environ.* **2019**, *658*, 1514–1522. [[CrossRef](#)] [[PubMed](#)]
29. Liu, Y.; Guo, L.; Huang, Z.; Wu, G.; Lopez-Vicente, M. Root morphological characteristics and soil water infiltration capacity in semi-arid artificial grassland soils. *Agric. Water Manag.* **2020**, *235*, 106153. [[CrossRef](#)]
30. Thompson, S.E.; Harman, C.J.; Heine, P.; Katul, G.G. Vegetation-infiltration relationships across climatic and soil type gradients. *J. Geophys. Res. Biogeophys.* **2015**, *115*, G02023. [[CrossRef](#)]
31. Dubbert, M.; Werner, C. Water fluxes mediated by vegetation: Emerging insights at the soil and atmosphere interfaces. *New Phytol.* **2018**, *221*, 1754–1763. [[CrossRef](#)]
32. Zhou, G.; Houlton, B.Z.; Wang, W.; Huang, W.; Xiao, Y.; Zhang, Q.; Liu, S.; Cao, M.; Wang, X.; Wang, S.; et al. Substantial reorganization of China's tropical and subtropical forests: Based on the permanent plots. *Glob. Chang. Biol.* **2014**, *20*, 240–250. [[CrossRef](#)] [[PubMed](#)]
33. Zhou, G.; Peng, C.; Li, Y.; Liu, S.; Zhang, Q.; Tang, X.; Liu, J.; Yan, J.; Zhang, D.; Chu, G. A climate change-induced threat to the ecological resilience of a subtropical monsoon evergreen broad-leaved forest in Southern China. *Glob. Chang. Biol.* **2013**, *19*, 1197–1210. [[CrossRef](#)]
34. Gaisberger, H.; Fremout, T.; Kettle, C.J.; Barbara, V.; Kemalasari, D.; Kanchanarak, T.; Thomas, E.; Serra-Diaz, J.M.; Svenning, J.C.; Slik, F.; et al. Tropical and subtropical Asia's valued tree species under threat. *Conserv. Biol.* **2021**, accepted. [[CrossRef](#)] [[PubMed](#)]
35. Zhou, Y.; Zhang, Z.; Zhu, B.; Cheng, X.; Yang, L.; Gao, M.; Kong, R. Maxent modeling based on CMIP6 models to project potential suitable zones for *Cunninghamia lanceolata* in China. *Forests* **2021**, *12*, 752. [[CrossRef](#)]
36. SFA. *China Forest Resources Report (2009–2013)*; State Forest Administration: Beijing, China, 2014; 75p.
37. Guan, F.; Tang, X.; Fan, S.; Zhao, J.; Peng, C. Changes in soil carbon and nitrogen stocks followed the conversion from secondary forest to Chinese fir and Moso bamboo plantations. *Catena* **2015**, *133*, 455–460. [[CrossRef](#)]
38. Penna, D.; Hopp, L.; Scandellari, F.; Allen, S.T.; Benettin, P.; Beyer, M.; Geris, J.; Klaus, J.; Marshall, J.D.; Schwendenmann, L.; et al. Ideas and perspectives: Tracing terrestrial ecosystem water fluxes using hydrogen and oxygen stable isotopes—Challenges and opportunities from an interdisciplinary perspective. *Biogeosciences* **2018**, *15*, 6399–6415. [[CrossRef](#)]
39. Sprenger, M.; Leistert, H.; Gimbel, K.; Weiler, M. Illuminating hydrological processes at the soil-vegetation-atmosphere interface with water stable isotopes. *Rev. Geophys.* **2016**, *54*, 674–704. [[CrossRef](#)]
40. Gazis, C.; Feng, X. A stable isotope study of soil water: Evidence for mixing and preferential flow paths. *Geoderma* **2004**, *119*, 97–111. [[CrossRef](#)]
41. Wan, H.; Liu, W. An isotope study ( $\delta^{18}\text{O}$  and  $\delta\text{D}$ ) of water movements on the Loess Plateau of China in arid and semiarid climates. *Ecol. Eng.* **2016**, *93*, 226–233. [[CrossRef](#)]
42. Xu, Q.; Liu, S.; Wan, X.; Jiang, C.; Song, X.; Wang, J. Effects of rainfall on soil moisture and water movement in a subalpine dark coniferous forest in southwestern China. *Hydrol. Process.* **2012**, *26*, 3800–3809. [[CrossRef](#)]
43. Wang, Q.; Wang, S.; Yu, H. Comparisons of litterfall, litter decomposition and nutrient return in a monoculture *Cunninghamia lanceolata* and a mixed stand in southern China. *For. Ecol. Manag.* **2008**, *255*, 1210–1218. [[CrossRef](#)]
44. Zhao, P.; Tang, X.; Zhao, P.; Zhang, W.; Tang, J. Mixing of event and pre-event water in a shallow Entisol in sloping farmland based on isotopic and hydrometric measurements, SW China. *Hydrol. Process.* **2016**, *30*, 3478–3493. [[CrossRef](#)]
45. Lin, G.; Phillips, S.L.; Ehleringer, J.R. Monsoonal precipitation responses of shrubs in a cold desert community on the Colorado Plateau. *Oecologia* **1996**, *106*, 8–17. [[CrossRef](#)] [[PubMed](#)]
46. West, A.G.; Patrickson, S.J.; Ehleringer, J.R. Water extraction times for plant and soil materials used in stable isotope analysis. *Rapid Commun. Mass Sp.* **2006**, *20*, 1317–1321. [[CrossRef](#)]
47. White, J.; Cook, E.R.; Lawrence, J.R.; Broecker, W.S. The D/H ratios of sap in trees: Implications for water sources and tree ring D/H ratios. *Geochim. Cosmochim. Acta* **1985**, *49*, 237–246. [[CrossRef](#)]
48. Bai, Y.; Zhou, Y.; Du, J.; Zhang, X.; Di, N. Effects of a broadleaf-oriented transformation of coniferous plantations on the hydrological characteristics of litter layers in subtropical China. *Glob. Ecol. Conserv.* **2020**, *25*, e01400. [[CrossRef](#)]
49. Özcan, M.; Gökbulak, F.; Hizal, A. Enclosure effects on recovery of selected soil properties in a mixed broadleaf forest recreation site. *Land Degrad. Dev.* **2013**, *24*, 266–276. [[CrossRef](#)]
50. Dunkerley, D. Percolation through leaf litter: What happens during rainfall events of varying intensity? *J. Hydrol.* **2015**, *525*, 737–746. [[CrossRef](#)]
51. Meier, I.C.; Knutzen, F.; Eder, L.M.; Müller-Haubold, H.; Leuschner, C. The deep root system of *Fagus sylvatica* on sandy soil: Structure and variation across a precipitation gradient. *Ecosystems* **2017**, *21*, 280–296. [[CrossRef](#)]
52. Wu, H.; Li, X.Y.; Jiang, Z.; Chen, H.; Zhang, C.; Xiao, X. Contrasting water use pattern of introduced and native plants in an alpine desert ecosystem, Northeast Qinghai–Tibet Plateau, China. *Sci. Total Environ.* **2016**, *542*, 182–191. [[CrossRef](#)]
53. Crockford, R.H.; Richardson, D.P. Partitioning of rainfall into throughfall, stemflow and interception: Effect of forest type, ground cover and climate. *Hydrol. Process.* **2015**, *14*, 2903–2920. [[CrossRef](#)]

54. Daly, E.; Porporato, A. A review of soil moisture dynamics: From rainfall infiltration to ecosystem response. *Environ. Eng. Sci.* **2005**, *22*, 9–24. [[CrossRef](#)]
55. Geroy, I.J.; Gribb, M.M.; Marshall, H.P.; Chandler, D.G.; Benner, S.G.; Mcnamara, J.P. Aspect influences on soil water retention and storage. *Hydrol. Process.* **2011**, *25*, 3836–3842. [[CrossRef](#)]
56. Sun, D.; Yang, H.; Guan, D.; Yang, M.; Wu, J.; Yuan, F.; Jin, C.; Wang, A.; Zhang, Y. The effects of land use change on soil infiltration capacity in China: A meta-analysis. *Sci. Total Environ.* **2018**, *626*, 1394–1401. [[CrossRef](#)]
57. Yinglan, A.; Wang, G.; Liu, T.; Shrestha, S.; Xue, B.; Tan, Z. Vertical variations of soil water and its controlling factors based on the structural equation model in a semi-arid grassland. *Sci. Total Environ.* **2019**, *691*, 1016–1026.
58. Gao, X.; Li, H.; Zhao, X.; Ma, W.; Wu, P. Identifying a suitable revegetation technique for soil restoration on water-limited and degraded land: Considering both deep soil moisture deficit and soil organic carbon sequestration. *Geoderma* **2018**, *319*, 61–69. [[CrossRef](#)]
59. Leung, A.; Garg, A.; Coe, J.; Ng, C.; Hau, C. Effects of the roots of *Cynodon dactylon* and *Schefflera heptaphylla* on water infiltration rate and soil hydraulic conductivity. *Hydrol. Process.* **2015**, *29*, 3342–3354. [[CrossRef](#)]
60. Marin, C.T.; Bouten, W.; Sevink, J. Gross rainfall and its partitioning into throughfall, stemflow and evaporation of intercepted water in four forest ecosystems in western Amazonia. *J. Hydrol.* **2000**, *237*, 40–57. [[CrossRef](#)]
61. Liu, Z.; Ma, D.; Hu, W.; Li, X. Land use dependent variation of soil water infiltration characteristics and their scale-specific controls. *Soil Till. Res.* **2018**, *178*, 139–149. [[CrossRef](#)]
62. Zhao, S.W.; Zhao, Y.G.; Wu, J.S. Quantitative analysis of soil pores under natural vegetation successions on the Loess Plateau. *Sci. China Earth Sci.* **2010**, *53*, 617–625. [[CrossRef](#)]
63. Alaoui, A. Modelling susceptibility of grassland soil to macropore flow. *J. Hydrol.* **2015**, *525*, 536–546. [[CrossRef](#)]
64. Zhi, W.; Hua, Z.; Jrs, D.; Zoa, B. Plant functional diversity mediates indirect effects of land-use intensity on soil water conservation in the dry season of tropical areas. *For. Ecol. Manag.* **2021**, *480*, 118646.
65. Sun, J.; Yu, X.; Wang, H.; Jia, G.; Chen, J. Effects of forest structure on hydrological processes in China. *J. Hydrol.* **2018**, *561*, 187–199. [[CrossRef](#)]
66. Huang, Z.; Tian, F.; Wu, G.; Liu, Y.; Dang, Z. Legume grasslands promote precipitation infiltration better than Gramineous grasslands in the arid regions. *Land Deg. Dev.* **2016**, *28*, 309–316. [[CrossRef](#)]
67. Hudek, C.; Stanchi, S.; D'Amico, M.E.; Freppaz, M. Quantifying the contribution of the root system of alpine vegetation in the soil aggregate stability of moraine. *J. Soil Water Conserv.* **2017**, *5*, 36–42. [[CrossRef](#)]
68. Bormann, H.; Klaassen, K. Seasonal and land use dependent variability of soil hydraulic and soil hydrological properties of two Northern German soils. *Geoderma* **2008**, *145*, 295–302. [[CrossRef](#)]
69. Clemmensen, K.E.; Bahr, A.; Ovaskainen, O.; Dahlberg, A.; Ekblad, A.; Wallander, H.; Stenlid, J.; Finlay, R.D.; Wardle, D.A.; Lindahl, B.D. Roots and associated fungi drive long-term carbon sequestration in boreal forest. *Science* **2013**, *339*, 1615–1618. [[CrossRef](#)]
70. Perie and Ouimet. Organic carbon, organic matter and bulk density relationships in boreal forest soils. *Can. J. Soil* **2008**, *88*, 315–325. [[CrossRef](#)]
71. Yan, T.; Wang, Z.; Liao, C.; Xu, W.; Wan, L. Effects of the morphological characteristics of plants on rainfall interception and kinetic energy. *J. Hydrol.* **2020**, *592*, 106689. [[CrossRef](#)]
72. Wang, B.; Verheyen, K.; Baeten, L.; Smedt, P.D. Herb litter mediates tree litter decomposition and soil fauna composition. *Soil Biol. Biochem.* **2020**, *152*, 10863. [[CrossRef](#)]
73. Mishra, S.; Singh, K.; Sahu, N.; Singh, S.N.; Manika, N.; Chaudhary, L.B.; Jain, M.K.; Kumar, V.; Behera, S.K. Understanding the relationship between soil properties and litter chemistry in three forest communities in tropical forest ecosystem. *Environ. Monit. Assess.* **2019**, *191*, 797. [[CrossRef](#)] [[PubMed](#)]
74. Jin, T.T.; Fu, B.J.; Liu, G.H.; Wang, Z. Hydrologic feasibility of artificial forestation in the semi-arid Loess Plateau of China. *Hydrol. Earth Syst. Sci.* **2011**, *15*, 2519–2530. [[CrossRef](#)]
75. Robichaud, P.R. Fire effects on infiltration rates after prescribed fire in Northern Rocky Mountain forests, USA. *J. Hydrol.* **2000**, *231*, 220–229. [[CrossRef](#)]
76. Pavão, L.L.; Sanches, L.; Júnior, O.P.; Spolador, J. The influence of litter on soil hydro-physical characteristics in an area of Acuri palm in the Brazilian Pantanal. *Ecohydrol. Hydrobiol.* **2019**, *19*, 642–650. [[CrossRef](#)]